The influence of γ-fibre texture on the grain boundary character distribution of an IF-steel

Hossein Beladi [a],[*], Vahid Tari [b], Anthony D. Rollett [c], Gregory S. Rohrer [c]

[a] *Institute for Frontier Materials, Deakin University, Geelong, VIC 3216, Australia*
[b] *ATI Specialty Materials, Monroe, NC, 28111, United States*
[c] *Department of Materials Science and Engineering, Carnegie Mellon University, Pittsburgh, PA 15213-3890, United States*

ARTICLE INFO

ABSTRACT

The current study revealed that the development of γ-fibre texture in IF-steel through static recrystallisation alters the distribution of grain boundary misorientations and plane orientations. In the initial transformed condition, the grain boundary plane distribution has a maximum at the (110) orientation. However, as the intensity of the γ-fibre texture increased, the maximum shifted to (111) and intensified. Furthermore, the presence of γ-fibre texture gradually increased the low angle boundary population at the expense of high angle boundaries, leading to a nearly uniform misorientation angle distribution. A calculation of the disorientation distribution assuming random orientations along the γ-fibre showed a flat distribution in the domain from 0 to 60°, consistent with the observations. The presence of γ-fibre texture changed the intensity, but not the shape of the grain boundary distribution at $\sum 3 = 60°/[111]$, which displayed maxima at low energy {112} symmetric tilt boundaries.

Grain boundaries are active microstructure components in polycrystalline materials whose characteristics influence materials properties (i.e., strength, toughness and corrosion). Since the mid-1980s, research has been conducted with the goal of controlling the grain boundary network to improve the material performance [1–8]. Here, we use the phrase grain boundary network to refer to the populations of different types of boundaries, distinguished by lattice misorientation and grain boundary plane orientation, and their connectivity. A number of approaches are now used to manipulate the grain boundary network, utilising distinct microstructure evolution mechanisms such as recrystallisation and phase transformation depending on the alloy composition and processing route. These approaches include iterative recrystallisation [2], alloy composition modification [2,3,4], phase transformation mechanism control (i.e., shear vs diffusion) [3,5,6], variant selection [3,4,7] and texture development [6,8,9,10]. Amongst these different approaches, the role of orientation texture on the grain boundary network has received less attention, despite the fact that controlling the grain orientation distribution has predictable consequences on the distribution of lattice misorientations [10] and the grain boundary plane distribution [11].

Interstitial free (IF) steel is technologically important because, when γ-fibre texture (<111>//ND-fibre) is developed through the control of cold rolling and annealing (recrystallisation), it offers outstanding deep drawability and formability [12]. Previous work indicates that the γ-fibre alters the grain boundary network, promoting boundaries with the (111) orientation [6], rather than the (110) close packed plane orientation which is usually found in body centred cubic materials (e.g., ferrite) and has the lowest energy [13]. In addition, the γ-fibre leads to approximately a uniform distribution of misorientation angles, as expected for a texture with a single degree of freedom [6]. Garcia and Vaudin presented an analytical approach, utilising the orientation distribution function (ODF), to calculate the misorientation probability distribution for a material with a fibre texture [10]. Their calculation predicts that the fibre texture promotes two shallow peaks at the highest and lowest misorientation angle regimes and a constant distribution in between [10]. Their calculation, however, ignored crystal symmetries, producing a misorientation distribution with a domain of rotation angles from 0 to π. With crystal symmetry, the domain of unique disorientations for the <111>//ND texture is limited to be between 0 and π/3.

The current study initially aims to evaluate the effect of γ-fibre texture strength in IF-steel on the grain boundary network characteristics by altering the amount of cold reduction (0 through 80%) prior to the annealing treatment. This process enables us to progressively alter the strength of γ-fibre texture and closely monitor its effect on the grain

---

boundary character distribution. The results were then interpreted by comparing with a calculation of the ideal disorientation distribution for the case of ideal γ-fibre texture, employing all orientations belonging to the γ-fibre uniformly and crystal symmetry.

In the current investigation, the as-received material was a hot rolled IF-steel slab with a thickness of 25 mm, having a composition of 0.003C-0.13Mn-0.08Ti-0.03Al-0.004 N (wt%). The slab was initially subjected to a multi-pass rolling process in the temperature range of 1200 °C to 1100 °C followed by air cooling to obtain the steel with a thickness of 5 mm, hereafter called the initial/transformed condition (i.e., 0% cold rolling). The material was then cold rolled to reductions of 30%, 60% and 80%, followed by annealing at 800 °C for 60 min, 30 min and 15 min, respectively in a fluid bed furnace in flowing nitrogen gas.

The microstructure was examined using electron backscatter diffraction (EBSD) using a FEGSEM Quanta 3D FEI scanning electron microscope operated at 20 kV, equipped with a fully automated EBSD device. Data acquisition and post processing were conducted using the TexSEM Laboratories, Inc. software (TSL). EBSD samples were prepared using standard mechanical polishing, finished with a colloidal silica slurry polish. Multiple EBSD maps were acquired at two cross sections, namely the rolling direction-normal direction (RD-ND) section and the rolling direction-transverse direction (RD-TD) section, to minimise the texture bias for the grain boundary characterisation. The EBSD step size was 1 μm on a hexagonal grid. At least 50,000 grain boundary line traces were collected for each condition so that a stereological interpretation of the data produces a reliable estimate of the distribution of grain boundary planes using the so called 5-parameter characterisation approach [14].

The IF-steel microstructure after multi-pass deformation at 1200 °C to 1100 °C followed by air-cooling revealed a relatively coarse equiaxed grain structure with an average of size of 81.3 ± 1.9 μm (Fig. 1a). Parent austenite-to-ferrite (martensite/bainite) phase transformations in steels follow specific crystallographic orientation relationships (OR), varying from Kurdjumov-Sachs (K-S) and Nishiyama-Wasserman (N-W), which, however, only differ by ~5.26° [16]. Recently, the orientation relationship of parent austenite and martensite was evaluated in a low carbon content steel (0.04 wt%), showing that most austenite grains closely follow the K-S OR upon transformation [5]. Due to the ultralow carbon content in the current steel (i.e., 0.003 wt%C), it is, therefore, assumed that the transformation follows the K-S OR. Accordingly, the dominant Cube texture developed in recrystallised parent austenite during multi-pass hot deformation in a range of 1200–1100 °C is mostly transformed into three main orientations, namely Goss (i.e., {110}<001>), rotated Cube (i.e., {100}<011>), and the rotated Goss (i.e., {110}<110>) upon the austenite-to-ferrite phase transformation [17]. This corresponds well with the overall texture of the fully ferritic microstructure transformed from the recrystallised austenite, displaying a relatively weak texture with ~3.5 MRD intensity (Fig. 2a).

Considering the K-S OR, each austenite grain theoretically transforms to as many as 24 different variants. The impingement of these variants results in the formation 16 distinct lattice misorientations (i.e., intervariant boundaries). Therefore, absent of variant bias, we expect misorientation angles of 10.5, 14.9, 20.6, 21.1, 47.1, 49.5, 50.5, 51.7, 57.2, and 60° based on the K-S OR [5]. This suggests that the misorientation angle distribution of ferrite resulting from the phase transformation should not display any misorientation angles <10° nor within
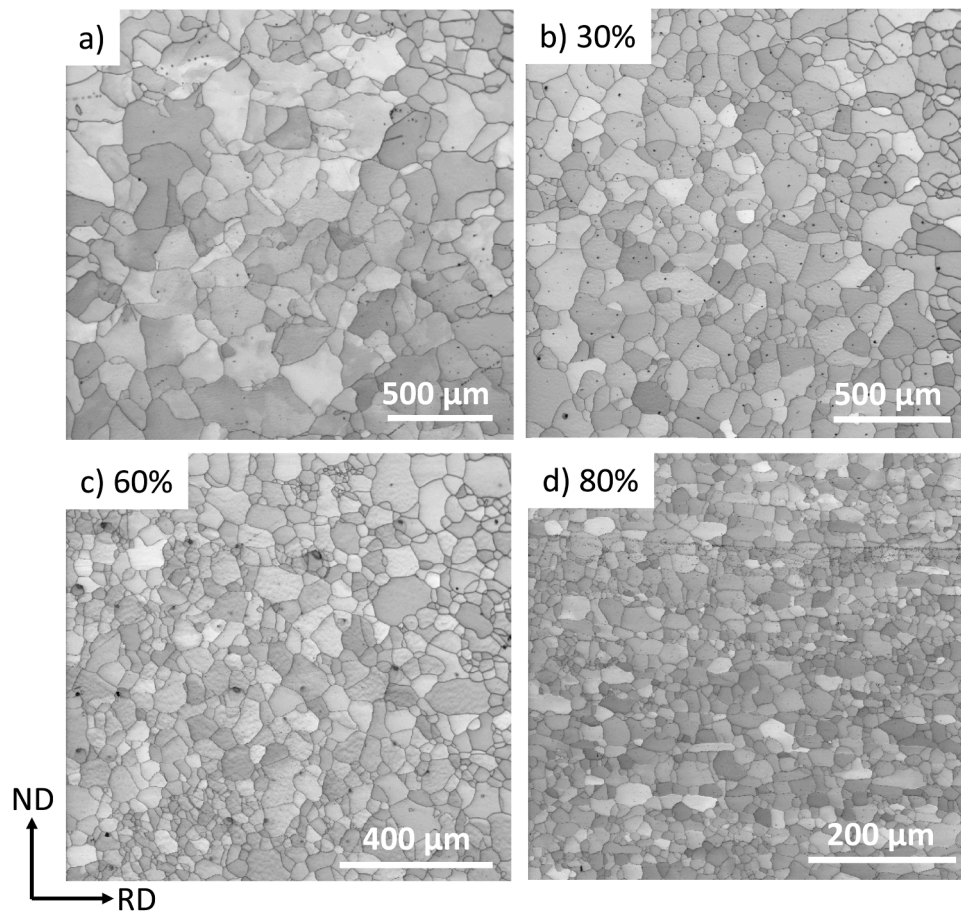
Fig. 1. The microstructure of IF steel subjected to different processing routes: a) ferrite transformed from recrystallised austenite, b,c and d) fully statically recrystallised ferrite formed through annealing of cold rolled material subjected to different reductions. RD and ND represent rolling direction and normal direction, respectively.
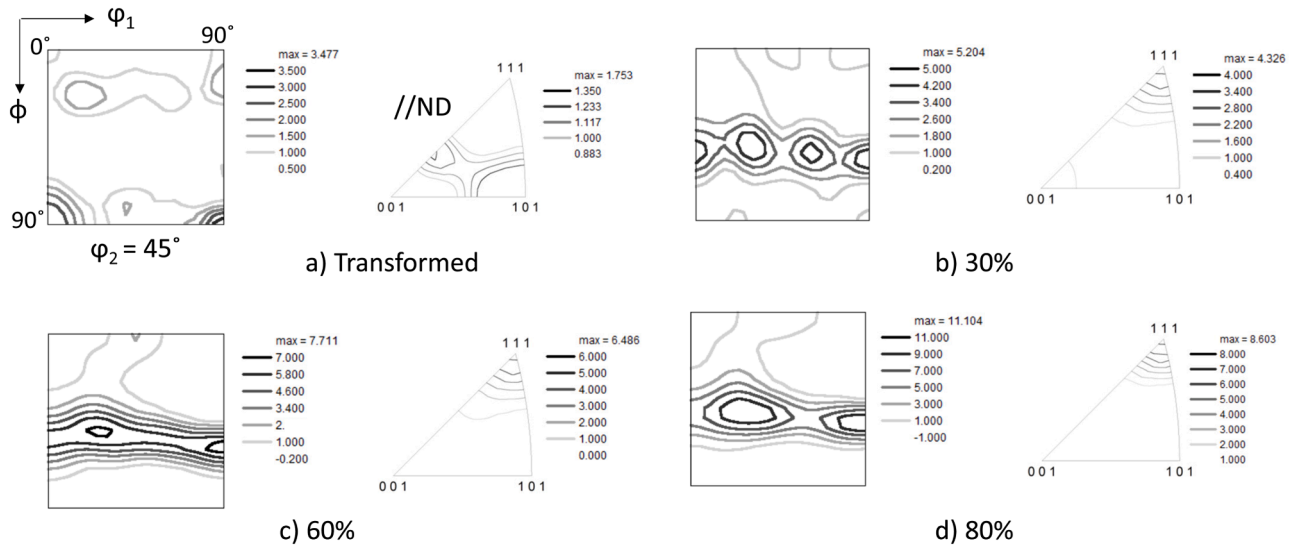
Fig. 2. The overall texture of IF steel subjected to different processing routes: a) ferrite transformed from recrystallised austenite, b,c and d) fully statically recrystallised ferrite formed through annealing of cold rolled material subjected to different reductions. ND is normal direction.

the range of 22 to 46°. However, the coarse ferrite misorientation angle distribution covered all possible misorientations from 5° (cut off value in the current study) up to 62.8° (maximum disorientation angle in the cubic-cubic fundamental zone). Note that the distribution revealed a sharp peak at 60° along with a moderate maximum in the range of 47–55°, which are well matched with those expected from the K-S OR. The presence of misorientations outside the theoretical values results from the impingement of variants on either side of prior austenite grain boundaries, which do not share any defined crystallographic relationship. Therefore, this impingement can yield any disorientation angle over the full range of 0 to 62.8°. A similar observation has been reported for other phase transformation products such as martensite [5] and bainite [18], though their population was much smaller than that of the current study. This could be due to the extent of refinement and number of variants formed during transformation in a given parent austenite grain during the martensitic/bainitic transformation. In the shear mechanism (e.g., martensite/bainite), the transformation takes place at a relatively low temperature regime (i.e., < 500 °C, depending on steel composition), leading to variant multiplications and microstructure refinement. Therefore, this results in a significant enhancement of the intervariant boundary populations. By contrast, the ferrite transformation takes place in a much higher temperature range (∼ 900 °C for the current steel), promoting the nucleation of a smaller number of variants (ferrite grains) within a given parent austenite grain. This leads to much coarser microstructure and lower fractions of intervariant boundaries because there are few ferrite grains for each parent grain. Consequently, the non K-S boundaries (misorientations) contribute more strongly to the misorientation distribution.

Cold deformation followed by annealing led to static recrystallisation of ferrite, resulting in an IF-steel with equiaxed grains. However, as with many metals, the ferrite grain size progressively decreased with increasing cold rolling reduction from 62.2 ± 1.5 μm at 30% reduction to 13.4 ± 1.2 μm at 80% reduction (Fig. 1). The cold rolling of IF-steel leads to the formation of shear bands consisting of dislocation cells across the microstructure [12]. This ultimately promotes a partial α-fibre (i.e., from {001}<110> to {111}<110>) and γ-fibre (i.e., from {111}<110> to {111}<112>) in the deformed material, referring to RD-fibre and ND-fibre, respectively [19]. During annealing, the deformed microstructure undergoes static recrystallisation through a preferred nucleation within the grains with the highest Taylor factor (i.e., high stored energy nucleation mechanism [20]), which prominently gives rise to the well-known γ-fibre recrystallisation texture (i.e.,

{111}<112> or ND-fibre).

This is well aligned with the current observation, where the static recrystallisation of ferrite after 30% cold rolling leads to a significant change in the overall texture in comparison with the transformed microstructure texture, promoting multiple peaks along the γ-fibre position with an intensity of 5.2 MRD (Fig. 2b). An increase in the cold rolling reduction progressively enhanced the γ-fibre intensity in the recrystallised microstructures from 7.7 MRD to 11.1 MRD for 60% and 80% cold reduction, respectively (Figs. 2c-d). In addition, the extent of cold rolling influenced the misorientation angle distribution of recrystallised ferrite (Fig. 3). At 30% reduction followed by recrystallisation, the development of γ-fibre texture led to a slight increase in the population of low-angle boundaries at the expense of boundaries with a 60° misorientation angle (Fig. 3b). An increase in the γ-fibre texture intensity after recrystallization of IF-steel subjected to higher reduction progressively enhanced the population of low angle boundaries, displaying a relatively flat misorientation angle distribution having two small peaks at ∼10° and 50° misorientation angles at 80% reduction (Fig. 3c-d).

To interpret the current observation, 1000 orientations are randomly chosen along the γ-fibre, ignoring sample symmetry, to examine the role of overall texture on the misorientation angle distribution (Fig. 4a). Here, the orientations are presented in terms of a set of Euler angles (i.e., φ_1, ϕ and φ_2), as defined by Bunge [21]. Therefore, the hypothetical orientations along the γ-fibre have their φ_1 randomly selected, varying from 0° through 360°, with fixed ϕ and φ_2 angles of 54.7° and 45°, respectively. Eq. (1) is used to calculate the misorientation angle resulting from the impingement of two orientations belonged to the γ-fibre.

$$\Delta g_{ij} = \left(O_m\, g_j\right)\left(O_l\, g_i\right)^{-1} \tag{1}$$

where Δg_{ij} is misorientation angle and g_i and g_j are ith and jth orientation of each neighbouring pair, respectively, both varying from 1 to 1000. O_l and O_m are the 24 cubic symmetry operators for g_i and g_j, respectively. From the set of 1152 equivalent misorientations (including switching symmetry), the result with minimum angle is selected, i.e., the disorientation. Here, it is assumed that these orientations meet each other only once, considering i is equal or smaller than j, as demonstrated in Fig. 4b. In addition, the length of boundary resulting from the impingement of each pair of orientations is fixed for all conditions. Therefore, it does not affect the misorientation angle distribution. Overall, the impingement of 1000 orientations leads to a total of 500,500 disorientations, which are
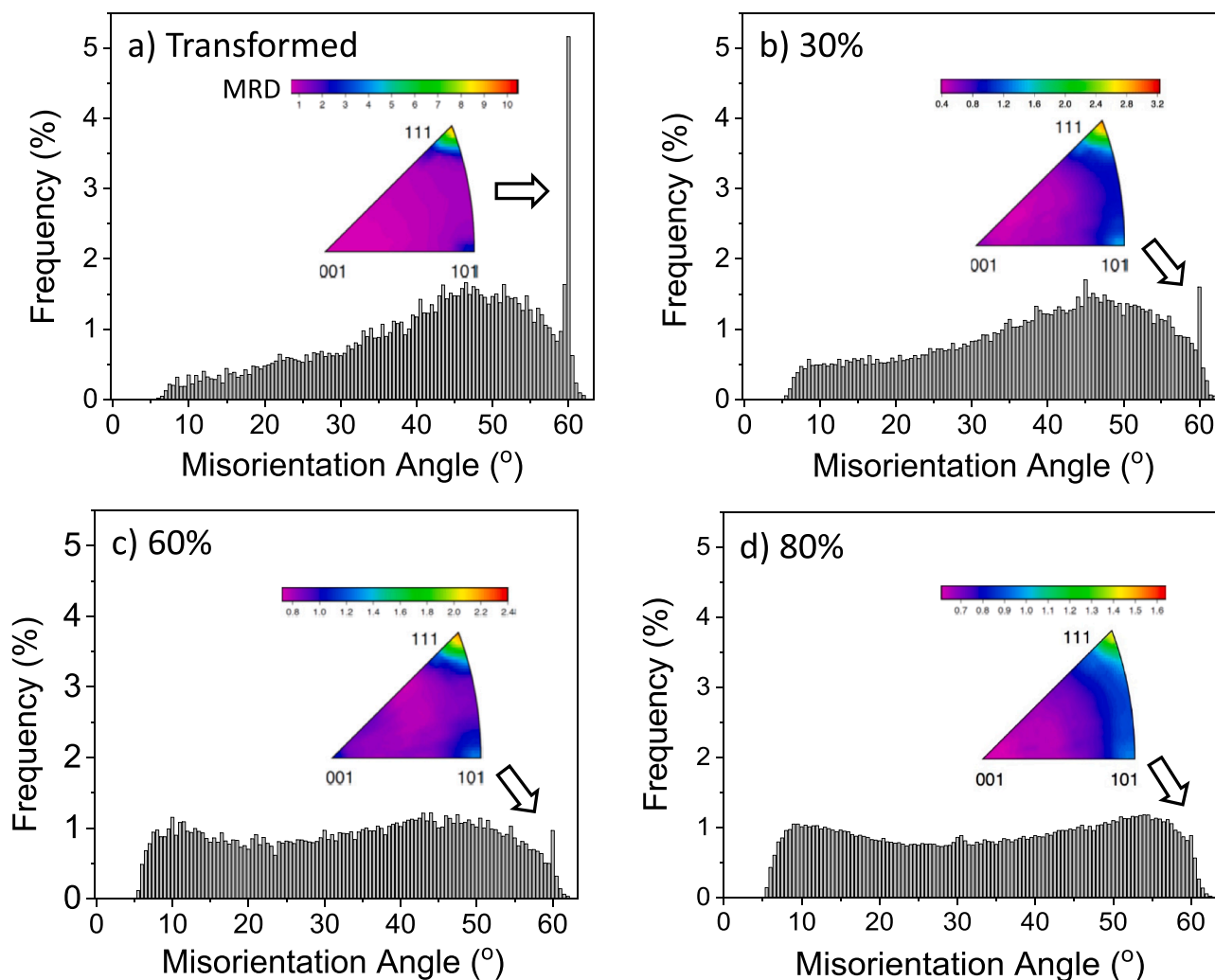
Fig. 3. Misorientation angle distribution along with the distribution of axes at rotation angle of 60° in a standard stereographic triangle for IF steel subjected to different processing routes: a) ferrite transformed from recrystallised austenite, b,c and d) fully statically recrystallised ferrite formed through annealing of cold rolled material subjected to different reductions. MRD represents multiples of a random distribution. (d) was adopted from [15].

presented in Fig. 4c as the disorientation angle distribution, discretised in bins with a width of 1° Here, the disorientation distribution is flat, except for some noise associated with the discretization (Fig. 4c). These spikes can be reduced by increasing the bin size and/or the number of γ-fibre orientations used in the calculation. As expected, all disorientations fall in the domain from 0 to 60°, the full range of distinguishable rotation angles about [111] (Fig. 4c). This indicates that a strong γ-fibre texture promotes the formation of all disorientations from 0° through 60° with a similar probability, leading to a uniform (top hat) distribution. This is also fully consistent with the trend in the current result, as the misorientation angle distribution progressively flattens out as the γ-fibre strengthens, i.e., increasing the low-angle boundary population at the expense of high-angle ones (specifically 60°, Fig. 3). However, the overall misorientation angle distribution at the strongest γ-fibre texture (i.e., ~11 MRD) revealed two relatively weak peaks at the lowest and highest misorientation range. In addition, a few boundaries with misorientation angles greater than 60° are still present in the distribution (Fig. 3d). These discrepancies arise from the finite spread of the data around the γ-fibre texture to include boundaries that are not part of the ideal γ-fibre texture (assumed in the calculation). These non-ideal boundaries broaden the disorientation distribution and create disorientations > 60°.

The relative grain boundary plane area distribution, irrespective of misorientation, is affected by the processing route (Fig. 5). The ferritic

microstructure resulting from the transformation of recrystallized austenite displayed a slight anisotropy having a peak at the (101) position with an intensity of 1.15 MRD (Fig. 5a). This suggests that the population of boundaries with (101) plane was 15% greater than expected in the random distribution. The (001) position was minimum with ~ 0.8 MRD and the (111) plane had ~1 MRD (Fig. 5a). The presence of a maximum at (101) is expected for the fully ferritic microstructure, as it represents a close packed plane in the bcc structure with a minimum energy arrangement [13]. The anisotropy of grain boundary plane distribution marginally decreased for the recrystallised ferrite after 30% cold rolling, however the position of the maximum changed to the (111) orientation with ~ 1.12 MRD (Fig. 5b). Further cold reduction progressively increased the anisotropy of the distribution, increasing the maximum at the (111) orientation to ~1.2 MRD and ~1.45 MRD at 60% and 80% cold rolling, respectively (Fig. 5c-d). It appears that the variation in the grain boundary plane distribution is closely related to the development of the γ-fibre texture in the ferritic microstructures (Fig. 2). In other words, the enhancement of γ-fibre texture leads to the promotion of boundaries with (111) plane orientation (Fig. 5).

The misorientation axes at 60° displayed a strong cluster around the ⟨111⟩ direction in the standard stereographic triangle for all ferritic microstructures (Fig. 3), suggesting the presence of Σ3 annealing twins (i.e., 60°/[111]) in all microstructures produced by different processing routes. The grain boundary plane distribution for 60°/[111] boundaries
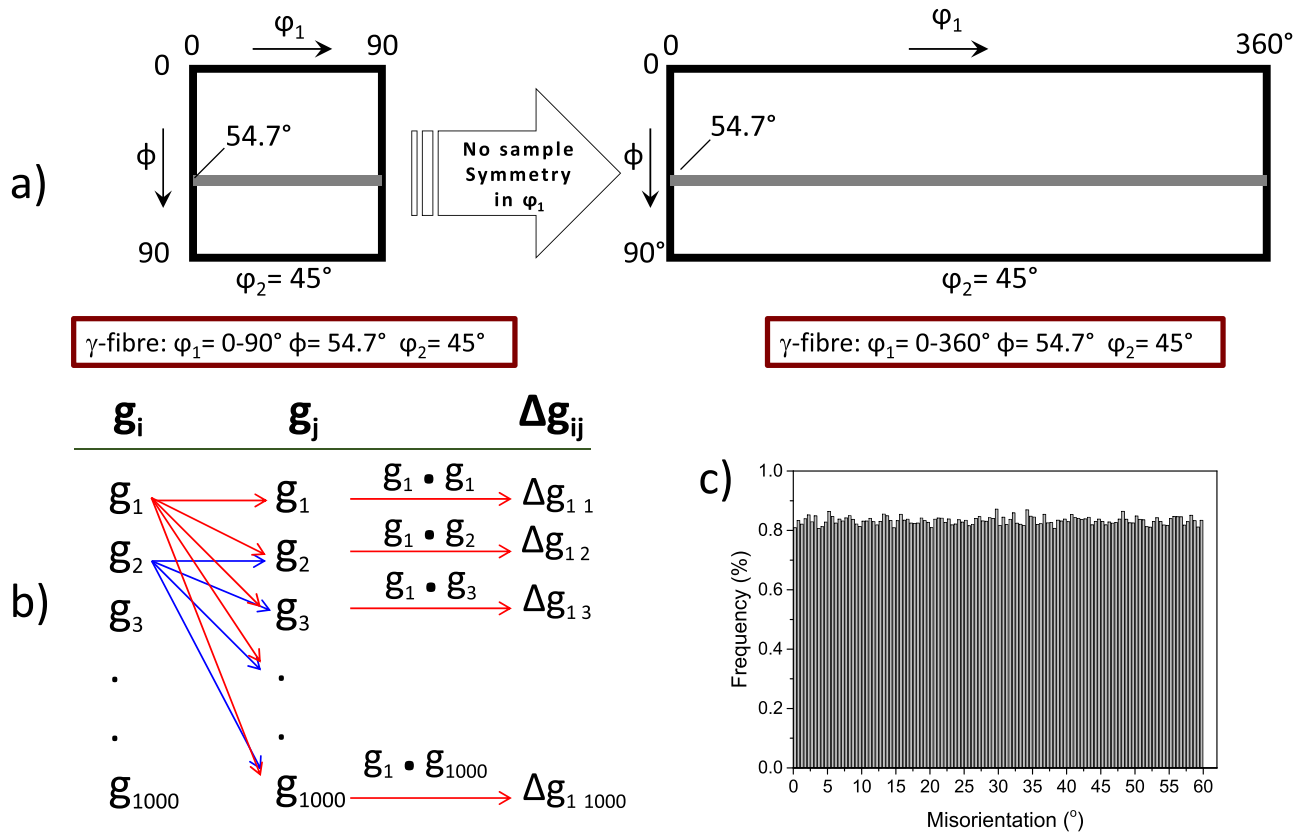
Fig. 4. Schematic representation of γ-fibre (i.e., <111>//ND) position in orientation distribution function at φ =45° cross section. b) Schematic demonstration of how disorientation angle is calculated each pair of 1000 orientations located on γ-fibre. c) the misorientation angle distribution resulted form impingement of each of pair of 1000 orientations related to the γ-fibre.
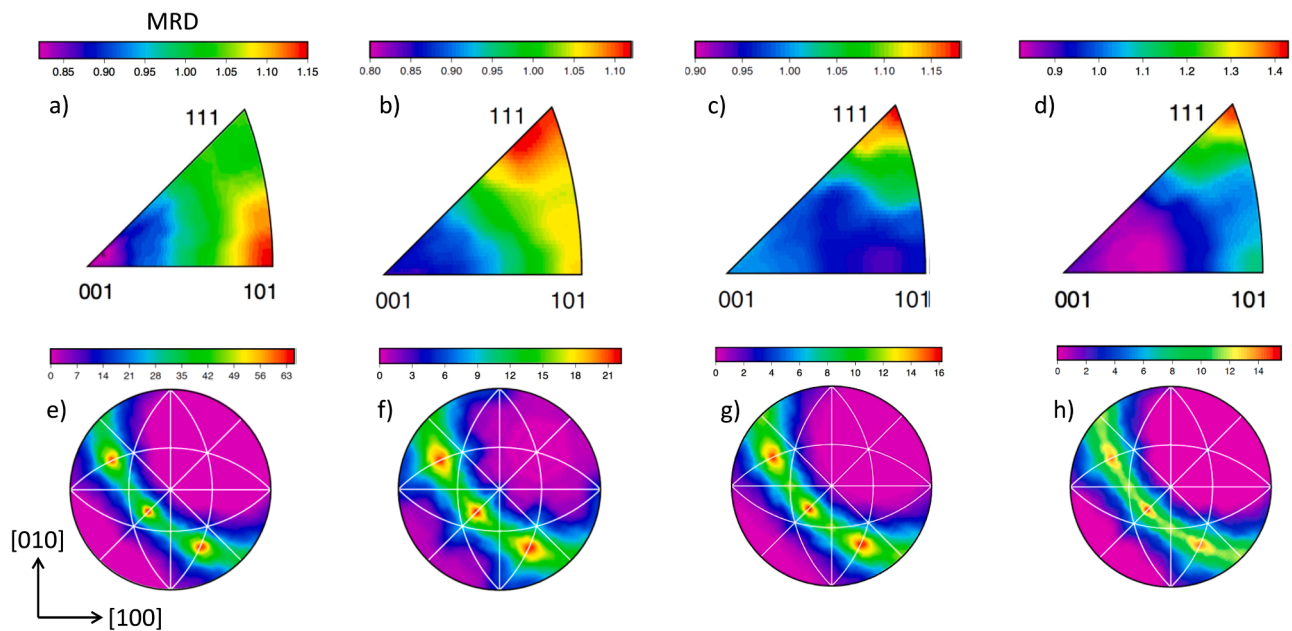

Fig. 5. (a-d) The relative area of grain boundary planes distribution, ignoring misorientation, and (e-h) the distribution of plane normals for $\sum 3 = 60°/[111]$ boundaries in IF steel subjected to different processing routes: a,e) ferrite transformed from recrystallised austenite, b-d and f-h) fully statically recrystallised ferrite formed through annealing of cold rolled material subjected to different reductions: b,f) 30%, c,g) 60% and d,h) 80%. MRD represents multiples of a random distribution. (d and h) were adopted from [15].

appeared along the tilt boundary zone, with the maxima at the (112) symmetric tilt boundary positions and minima at the (111) twist position for all ferritic microstructures (Fig. 5e-h). These distributions are

inversely correlated to the grain boundary energy distribution measured for the ferritic structure, where the (112) symmetric tilt boundaries and (111) pure twist emerged as minimum and maximum energy,

respectively [22]. Indeed, the {112}//{112} symmetric tilt grain boundaries represent coherent twin boundaries, which are commonly observed in materials with the bcc crystal structure. Although the processing route did not qualitatively alter the 60°/[111] distribution characteristics, the intensity of peaks noticeably decreased with the sharpening of the γ-fibre texture and the weakening of the 60° peak in misorientation, i.e., from 65 MRD for the transformed ferrite to ~22 MRD, ~16 and ~15 MRD for the recrystallised ferrite after 30%, 60% and 80% cold reduction, respectively (Fig. 5e-h). This implies that the overall texture influences the grain boundary population, rather than the shape of grain boundary plane orientation distribution for a given misorientation.

- The varying strength of the γ-fibre texture altered the distribution of misorientations and the grain boundary plane distributions in a deformed and recrystallized IF-steel.
- The varying γ-fibre texture did not change the shape of the grain boundary plane distribution at a fixed misorientation; at $\sum 3 = 60°/$[111] the maximum was at low energy {112} symmetric tilt boundaries independent of the processing route.
- The increasing strength of the γ-fibre gradually increased the low angle boundary population at the expense of high angle boundary population, leading to a more nearly uniform distribution of disorientations. This is in good agreement with a numerical calculation of the disorientation angle distribution for orientations spread along γ-fibre in the orientation distribution function, showing a flat distribution up to a maximum 60°

Declaration of Competing Interest

The authors declare that they have no known competing financial interests or personal relationships that could have appeared to influence the work reported in this paper.

References

[1] T. Watanabe, Trans. Japan Inst. Met. 27 (1986) 73.
[2] V. Randle, Acta Mater. 47 (1999) 4187.
[3] E. Farabi, V. Tari, P.D. Hodgson, G.S. Rohrer, H. Beladi, J. Mater. Sci. 55 (2020) 15299.
[4] V. Govindaraj, E. Farabi, S. Kada, P.D. Hodgson, R. Singh, G.S. Rohrer, H. Beladi, J. Alloy. Compd. 886 (2021), 161333.
[5] H. Beladi, G.S. Rohrer, A.D. Rollett, V. Tari, P.D. Hodgson, Acta Mater. 63 (2014) 86.
[6] H. Beladi, G.S. Rohrer, Metall. Mater. Trans. A 48 (2017) 2781.
[7] A. Mirzaei, R. Ghaderi, P.D. Hodgson, X. Ma, G.S. Rohrer, H. Beladi, J. Mater. Sci. 57 (2022) 8904.
[8] H. Beladi, E. Farabi, P.D. Hodgson, M.R. Barnett, G.S. Rohrer, D. Fabijanic, Philos. Mag. 102 (2022) 618.
[9] D.A. West, Adams B.L, Metall. Mater. Trans. A 28 (1997) 229.
[10] R.E. Garcia, M.D. Vaudin, Acta Mater. 55 (2007) 5728.
[11] C.S. Kim, A.D. Rollett, G.S. Rohrer, Scr. Mater. 54 (2006) 1005.
[12] M.D. Nave, M.R. Barnett, H. Beladi, ISIJ Int. 44 (2004) 1072.
[13] S.B. Lee, J.E. LeDonne, S.C.V. Lim, I.J. Beyerlein, A.D. Rollett, Acta Mater. 60 (2012) 1747.
[14] G.S. Rohrer, D.M. Saylor, B.E. Dasher, B.L. Adams, A.D. Rollett, P. Wynblatt, Z. für Metall. 95 (2004) 197.
[15] H. Beladi, G.S. Rohrer, Metall. Mater. Trans. A 44 (2013) 115.
[16] H.K.D.H. Bhedeshia, Bainite in Steels, 2nd ed, IOM Communications Ltd, London, 2001.
[17] M.P. Butron-Guillén, J.J. Jonas, ISIJ Int. 36 (1996) 68.
[18] B. Hutchinson, J. Komenda, G.S. Rohrer, H. Beladi, Acta Mater. 97 (2015) 380.
[19] L.A.I. Kestens, H. Pirgazi, Mater. Sci. Technol. 32 (2016) 1303.
[20] I. Samajdar, B. Verlinden, P. Van Houtte, D. Vanderschueren, Mater. Sci. Eng. A 238 (1997) 343.
[21] H.J. Bunge, Texture Analysis in Materials Science, Butterworth, London, 1993.
[22] H. Beladi, G.S. Rohrer, Acta Mater. 61 (2013) 1404.